8 p.

N64 23948

NASA CR 56287

Code 1 cat. 09

TRW SPACE TECHNOLOGY LABORATORIES
THOMPSON RAMO WOOLDRIDGE INC.
ONE SPACE PARK • REDONDO BEACH, CALIFORNIA

OTS PRICE

XEROX $ 3.60ph

MICROFILM $

STUDY OF SPACECRAFT
TRANSPONDER POWER AMPLIFIER

CONTRACT NAS5-3423

THIRD QUARTERLY REPORT

1 JANUARY 1964 to 31 MARCH 1964

PREPARED BY R. R. Cagnon
R. R. Cagnon

S. D. McCaskey
S. D. McCaskey

APPROVED BY R C Booton Jr.
Dr. R. C. Booton, Jr.
Director
Communication Laboratory

TABLE OF CONTENTS

ILLUSTRATIONS

I. INTRODUCTION

Advanced communication satellite studies as performed by STL for NASA indicate the need to extend transponder bandwidth capabilities in order to obtain the optimum balance between information rate, bandwidth and reasonable satellite output power.

Present satellite transponder configurations for RELAY, SYNCOM and TELSTAR use some form of a basic superhetrodyne receiver followed by a frequency upconverter and a traveling wave tube (TWT) power amplifier. The majority of the amplification takes place at some low intermediate frequency. While this technique has the advantage of being well within the "state-of-the-art", it has several disadvantages for future advanced communication satellites. The two most prominent disadvantages of present configurations are:

1. Such systems presently appear to be bandwidth limited to 40 or 50 mc.

2. Spurious responses inherent with the use frequency conversion and multiplication equipment introduce a definite problem when more than one wideband channel is envisioned.

It is the objective of this program to investigate a more advanced communication satellite transponder which will take advantage of RF amplification at or near the received or the transmitted frequency. This will be accomplished by utlizing a TWT in a re-entrant mode, coupled with a low noise front end and a possible output power amplifier.

II. TECHNICAL MEETINGS

Two technical meetings were held during this period. The first was held at STL on 12 through 14 February 1964 between technical personnel of NASA and STL. During the course of the meeting, the following persons were present:

W. Allen	NASA
S. McCaskey	STL
M. Davis	STL
R. Cagnon	STL
R. Boe	STL

The present status of the project was discussed as well as the course to be taken for future development.

The hardware effort in progress was shown which included the re-entrant amplifier portion of the transponder with the feedback loop closed, as well as the developmental laboratory area for the loop down-converter.

During the course of the meeting, the re-entrant loop was demonstrated with a wide band (16mc) FM television signal. This was accomplished by up-converting a 120 mc carrier to 6 gc and down-converting the 4 gc output signal. The base-band equipment used is similar to that used for RELAY system tests.

In addition to hardware considerations, the analytical aspects of the project were discussed. Further, the Hughes H-384 TWT, which may be available as government furnished equipment, was thoroughly discussed.

The second meeting was held at STL on 19 March 1964 between technical personnel of NASA and STL. During the course of the meeting, the following persons were present:

W. Allen	NASA
S. McCaskey	STL
M. Davis	STL
R. Cagnon	STL

Of the items covered, the following were of particular interest:

1. The present status of the loop down converter was discussed in detail as well as the course to be taken for future development.

2. The tunnel diode pre-amplifier characteristics were discussed with emphasis on rationale behind the selection.

3. The 384H and associated power supply, which will be used as the power amplifier, was discussed with emphasis on schedule. Mr. Allen stated that release to STL by 1 May would be feasible.

4. It was determined that Figure 3-24 of the Second Quarterly Report contained a calibration error and this curve is to be considered void.

III. INTERMODULATION DISTORTION ANALYSIS

Consider an input signal to the TWT consisting of two angle modulated carriers.

$$V_i(t) = A \cos \left[\omega_1 t + \phi_1 + \alpha_1\right] + B \cos \left[\omega_2 t + \phi_2(t) + \alpha_2\right] \qquad (1)$$

where A, B, ω_1 and ω_2 are constants, α_1 and α_2 are random variables, uniformly distributed from $-\pi$ to π, and $\phi_1(t)$ and $\phi_2(t)$ are sample functions of two independent wide-sense stationary Gaussian random processes having zero means. In particular $\phi_1(t)$ and $\phi_2(t)$ are taken to represent 300 channel FDM signals. This input may be considered as a two access system where each access consists of 300 telephone channels in frequency division multiplex. When such an input signal is amplified by the nonlinear characteristic of the TWT third and higher order intermodulation products are created which interfere with the desired carriers.

The effective noise caused by this interference, as seen at the received baseband, is expressed by the amount of psophometrically weighted noise present in any telephone channel due to the interference. The intermodulation noise due to the third order product nearest the desired carrier is given by*

$$N_{pw} = \left[\frac{3.1}{10^{0.25}} \left(\frac{f_b}{f_{drms}\sqrt{I}}\right)^2 \frac{\frac{C^2}{2} \times 10^{12}}{4\sqrt{3\pi}\sqrt{P_{eq}}\, f_{drms}}\right] \exp\left[\frac{-1}{12\, P_{eq}\, f^2_{drms}} (f-\Delta f)^2\right], \text{ pw (psoph)} \qquad (2)$$

where

N_{pw} = psophometrically weighted noise in the telephone channel located at frequency f

f_b = highest baseband frequency = 1.3 Mc for 300 channels

---

*The derivation of this equation is rather lengthy and will be presented in a later report. A portion of the derivation is presented in Appendix A which derives a procedure for determining the baseband interference spectrum.

f_{drms} = frequency deviation of carrier by an 800 cps test tone of 0 dbm0 power level

$C^2/2$ = power of third order product relative to the power of the desired carrier

I = pre-emphasis improvement factor
= 2.86 for 300 channels and 6 db per octave pre-emphasis

P_{eq} = equivalent noise power representing a multichannel FDM signal[1]
= $-15 + 10 \log_{10}(N_c)$, dbm0 $\quad N_c \geq 240$ channels

Δf = frequency separation of third order product and desired carrier

Substituting the appropriate constants for 300 channels, Equation (2) becomes

$$N_{pw} = 27.2 \times 10^3 \frac{C^2/2}{f_{drms}^3} \exp\left[\frac{-(f-\Delta f)^2}{114 f_{drms}^2}\right], \text{ pw (psoph)} \tag{3}$$

If the separation of the two carriers in the input signal is 25 Mc, Δf for the closest third-order product is also 25 Mc. Under these conditions the worst channel is the top channel located at 1.3 Mc. Figure 3-1 plots Equation (3) for this case with f_{drms} as a parameter. Equation (3) is valid for both third order products; however, the product located at f = 50 Mc is negligible. Figure 3-1 indicates that the amount of noise in the top channel due to third order interference with the original carriers is very small for reasonable intermodulation product levels unless the deviations are extremely high. For example, if the two input carriers each had a power of (P_s - 10), Figure 3-18 of the Second Quarterly Report shows the worst third order product to be down 28.5 db from the desired output tones for the MEC M5184 tube. From Figure 3-1 this corresponds to 14 pw of noise in the top or worst channel for a test tone deviation of 2 Mc.

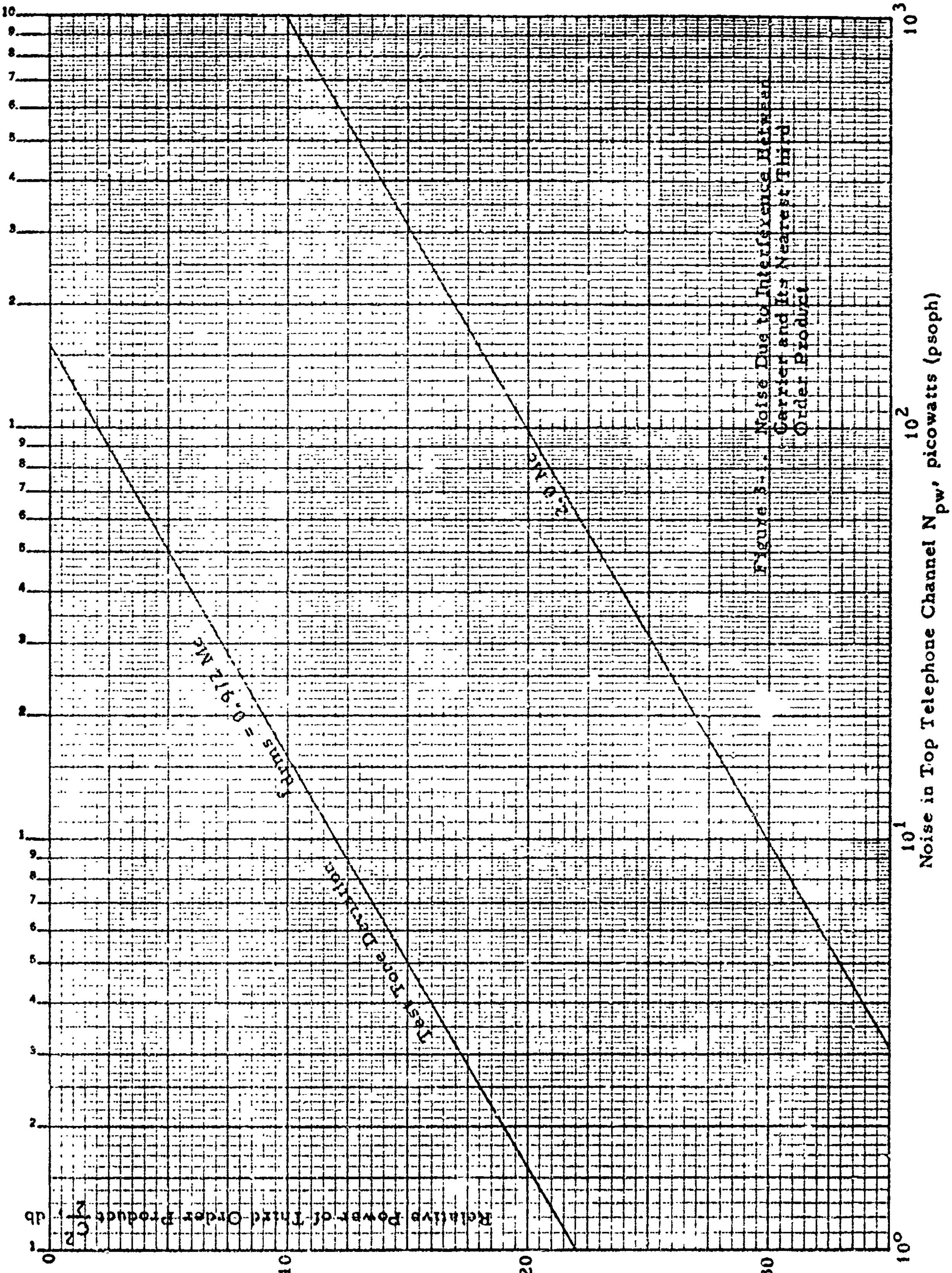

Figure 3 - Noise Due to Interference Between Carrier and Its Nearest Third Order Product

Now suppose that a third carrier is present at the input with frequency f_3 equal to $2f_2 - f_1$ or $2f_1 - f_2$; i.e., such that a third order product of f_1 and f_2 falls at the carrier frequency f_3. This would be the situation for the assumed frequency assignments (Figure 3-2) if f_1 and f_2 were separated by 50 Mc, 100 Mc, etc. This situation may be considered to be a worst case for interference. In this case, the noise in a telephone channel due to interference at f_3 by a third order product (of f_1 and f_2) may be found by setting $\Delta f = 0$ in Equation (3). The worst channel is now the lowest channel at f = 60 kc. Figure 3-3 is a plot of Equation (3) for this case with f_{drms} again a parameter.

The value of f_{drms} is normally chosen to achieve some specified thermal noise performance for the system; values used in Figures 3-1 and 3-3 correspond to the following qualities at receiver threshold.[2]

f_{drms}(Mc)	Thermal noise in top channel
0.200	380,000 pw
0.455	50,000 pw
0.674	18,750 pw
0.972	7,500 pw
2.00	1,230 pw

Thus, it may be seen from Figure 3-3 that the intermodulation noise due to a single third order product falling at a desired carrier frequency is small compared to the thermal noise assuming that pre-emphasis equalizes the thermal noise in all channels. However, a number of carriers at the input (up to 20 for the assumed frequency assignments) may produce several such products and the sum of the resulting intermodulation noises may not be negligible.

PLACEMENT OF COMMUNICATIONS BANDS

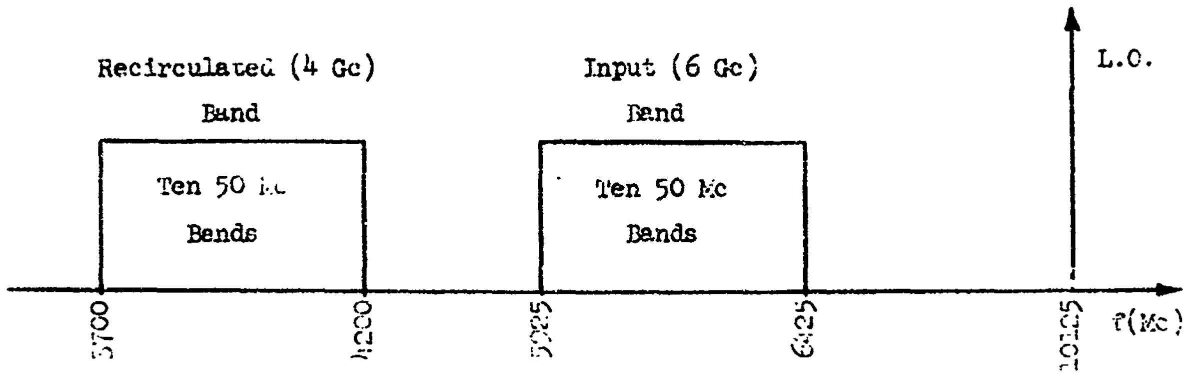

PLACEMENT OF CARRIERS IN 50 Mc BANDS

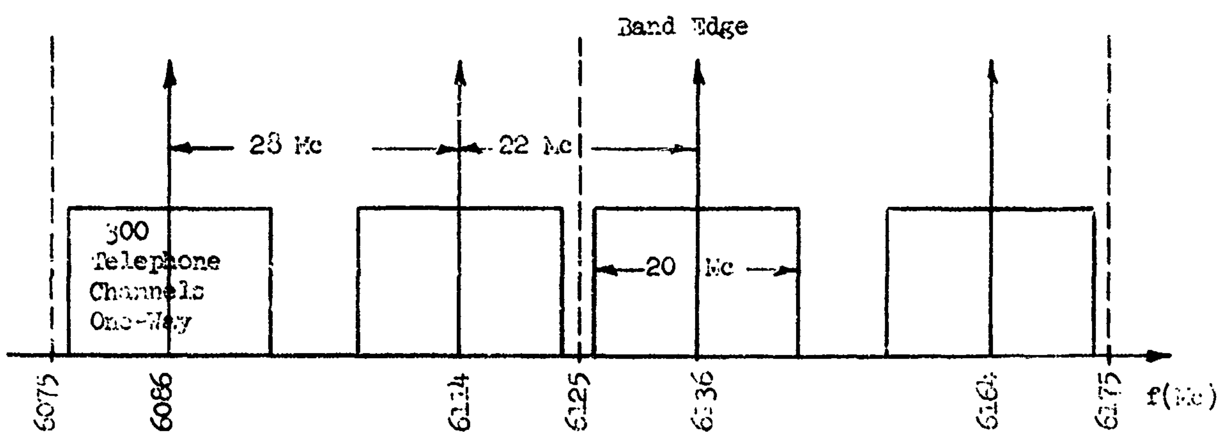

Figure 3-2 . Assumed Frequency Assignments

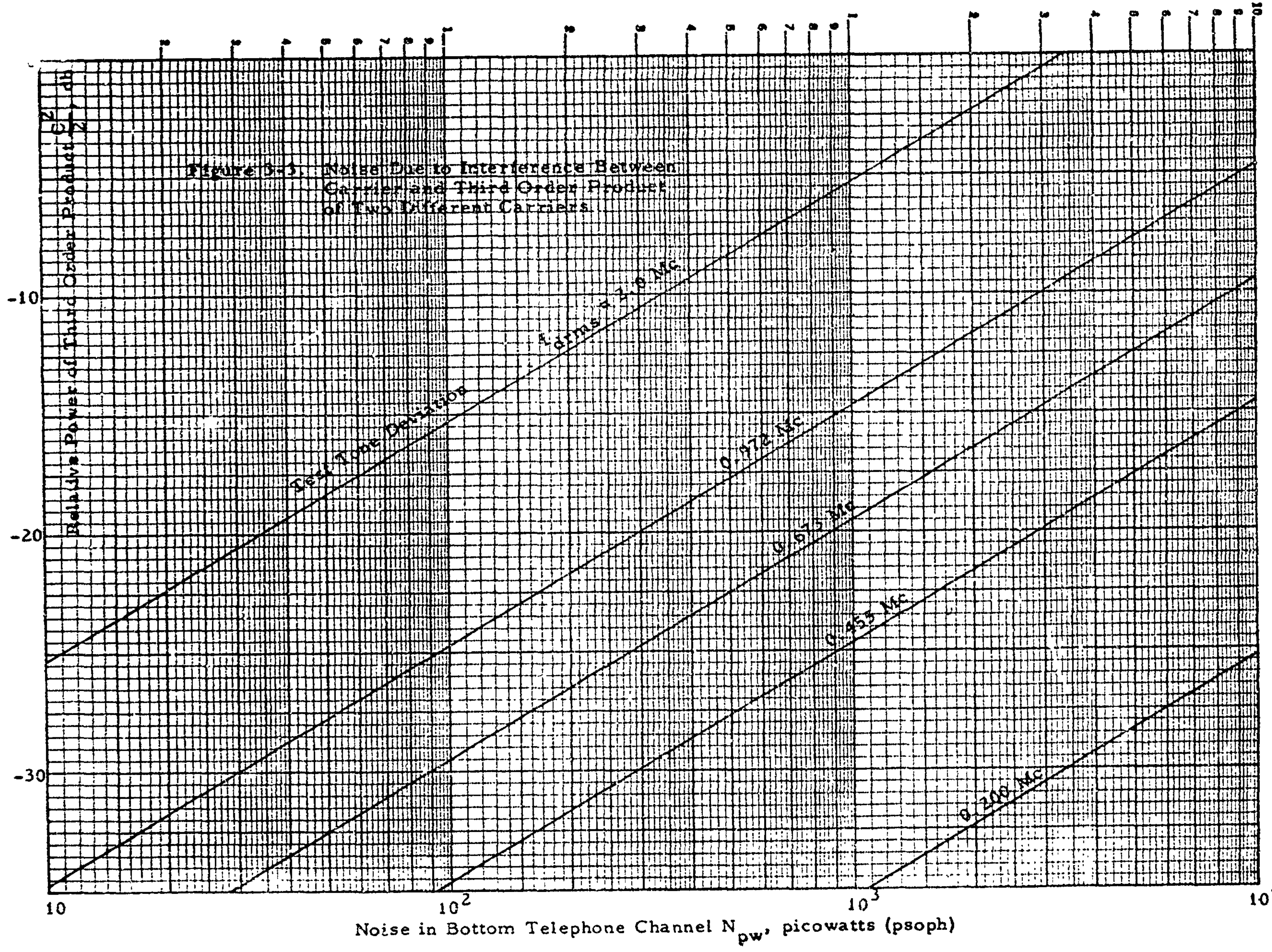

Figure 3-3. Noise Due to Interference Between Carrier and Third Order Product of Two Different Carriers

IV. RE-ENTRANT TRANSPONDER

The initial effort during this period was directed towards closing the re-entrant amplifier loop to verify the stability design criteria and to proceed with the loop amplifier evaluation. The loop components to be used in the final deliverable transponder were simulated with standard laboratory equipment to verify the integrity of each individual component specification prior to any financial commitment.

The major problem area during this period has been the progress of the down-converter development. The following section of this report has been devoted to the down-converter due to its unique requirements and importance to this program.

All other major items, which have been on order, are due during the month of May.

The re-entrant loop amplifier was closed during this period using the equipment shown in Figure 4-1. In this case, the diplexer was simulated by using high directivity coaxial couplers between filter junctions. An additional TWT amplifier was inserted in the feedback loop to simulate a no-loss loop to determine the loop stability under closed loop conditions.

The down-converter used for this test was of the varactor type but with poor bandwidth characteristics. By increasing the gain of the additional loop TWT however, the full 500 Mc bandwidth was simulated to determine the loop stability.

The test results showed a re-entrant amplifier gain of 72 db with a single frequency loop attenuation greater than 45 db, which is adequate to negate the possibility of oscillations.

The re-entrant amplifier was also demonstrated using the equipment shown in Figure 4-2.

The 120 Mc carrier is upconverted by the first mixer and the triple-stub tuner serves as a narrow band filter which allows only one sideband to pass. The modulated carr_er is then transmitted through the re-entrant loop amplifier and the resultant 4 gc signal is down-converted to 120 Mc and fed to the STL phase lock demodulator. The video is then fed to one side of the split screen TV monitor.

The pictures enclosed in ths section are indicative of the test results.

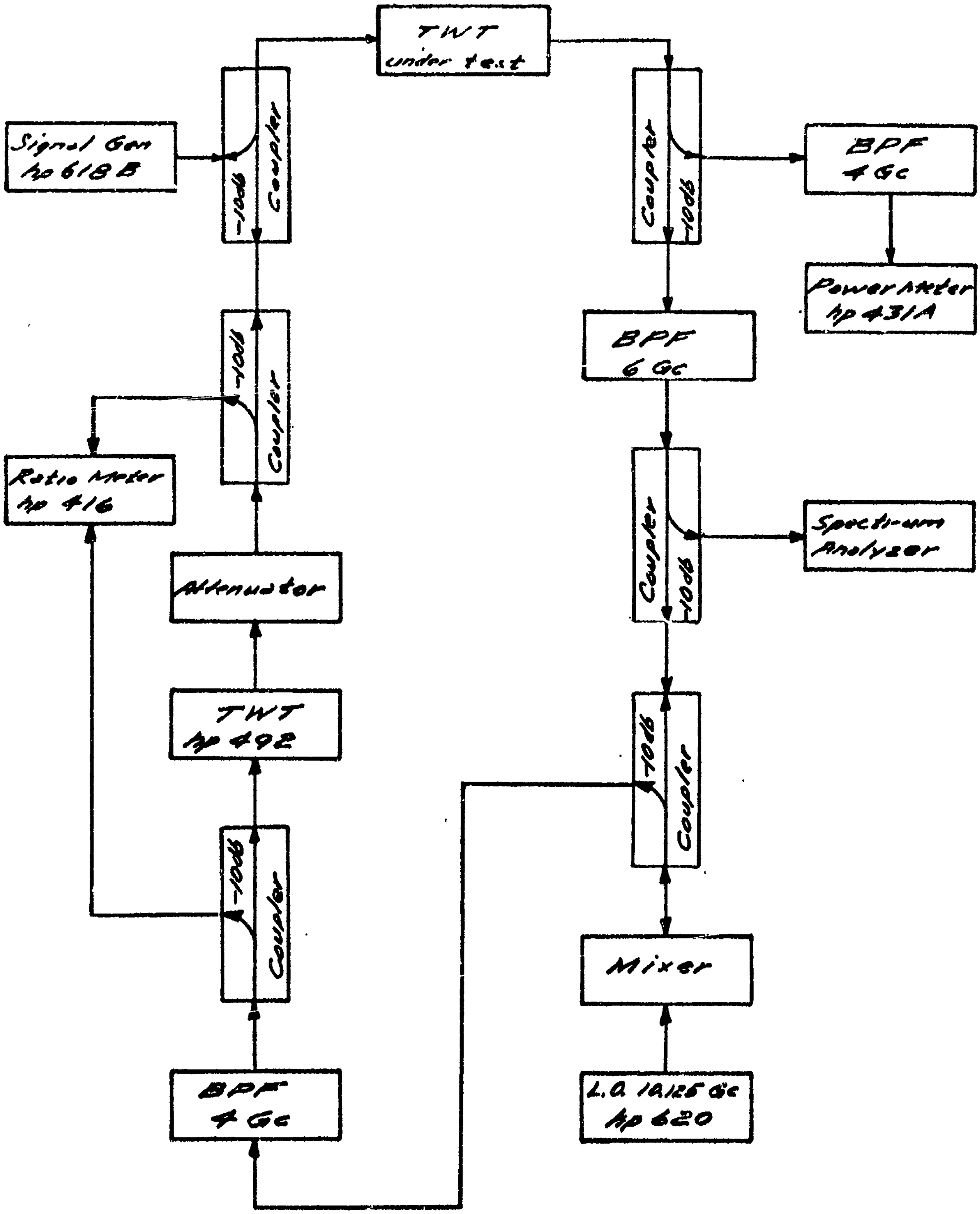

Figure 4.1. Closed Loop Test Block Diagram

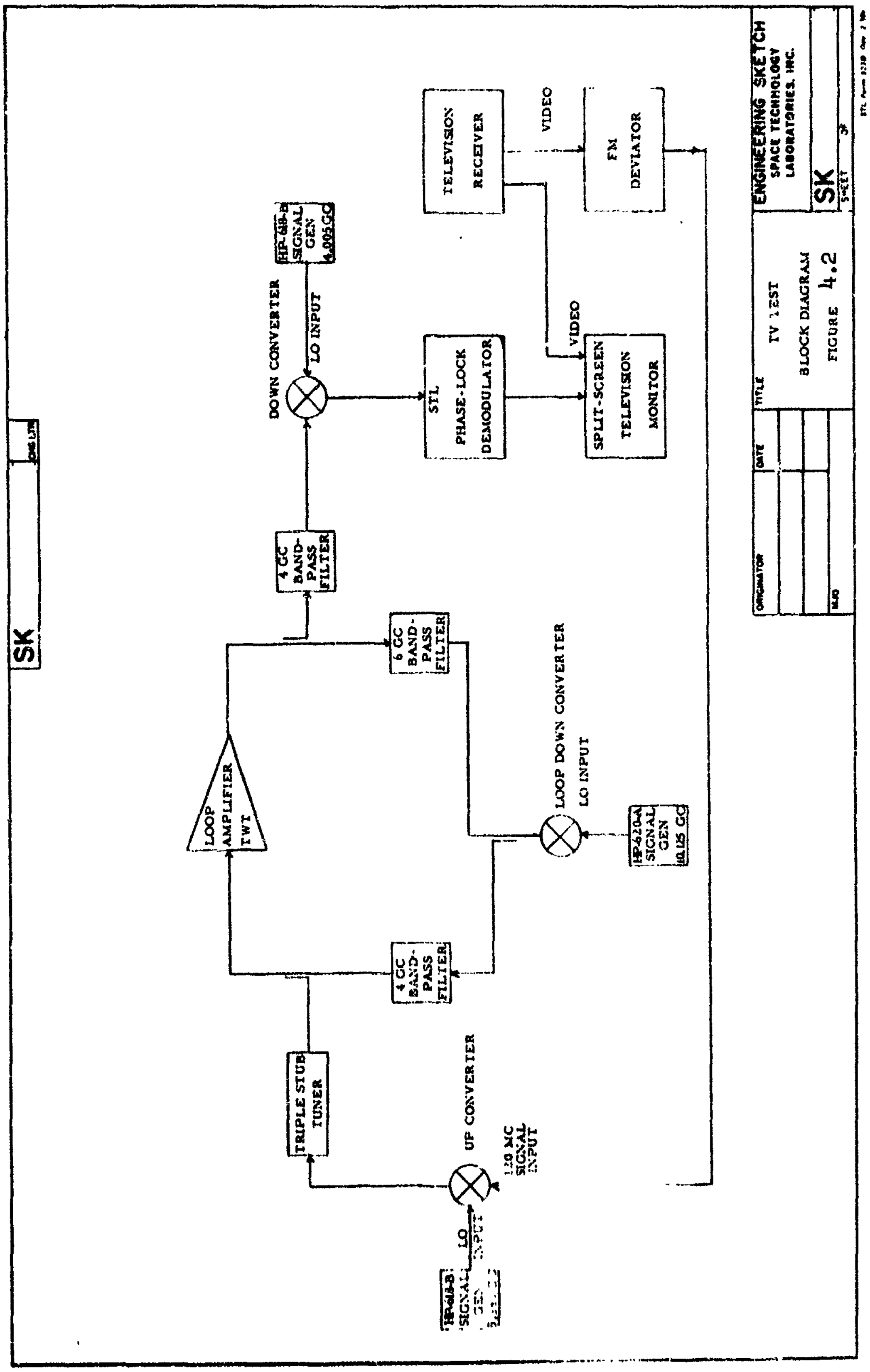
ENGINEERING SKETCH
SPACE TECHNOLOGY LABORATORIES, INC.
SK
TV TEST
BLOCK DIAGRAM
FIGURE 4.2
ORIGINATOR
DATE
TITLE
SHEET
TELEVISION RECEIVER
VIDEO
FM DEVIATOR
HP-618-B SIGNAL GEN 4.005 GC
DOWN CONVERTER
LO INPUT
STL PHASE-LOCK DEMODULATOR
VIDEO
SPLIT-SCREEN TELEVISION MONITOR
4 GC BAND-PASS FILTER
6 GC BAND-PASS FILTER
LOOP AMPLIFIER TWT
LOOP DOWN CONVERTER
LO INPUT
HP-620-A SIGNAL GEN 10.125 GC
4 GC BAND-PASS FILTER
TRIPLE STUB TUNER
UP CONVERTER
120 MC SIGNAL INPUT
LO INPUT
HP-618-B SIGNAL
SK

SPLIT SCREEN PRESENTATION OF WIDEBAND TV THROUGH RE-ENTRANT LOOP AND ORIGINAL VIDEO

SPLIT SCREEN PRESENTATION OF WIDEBAND TV THROUGH RE-ENTRANT LOOP AND ORIGINAL VIDEO

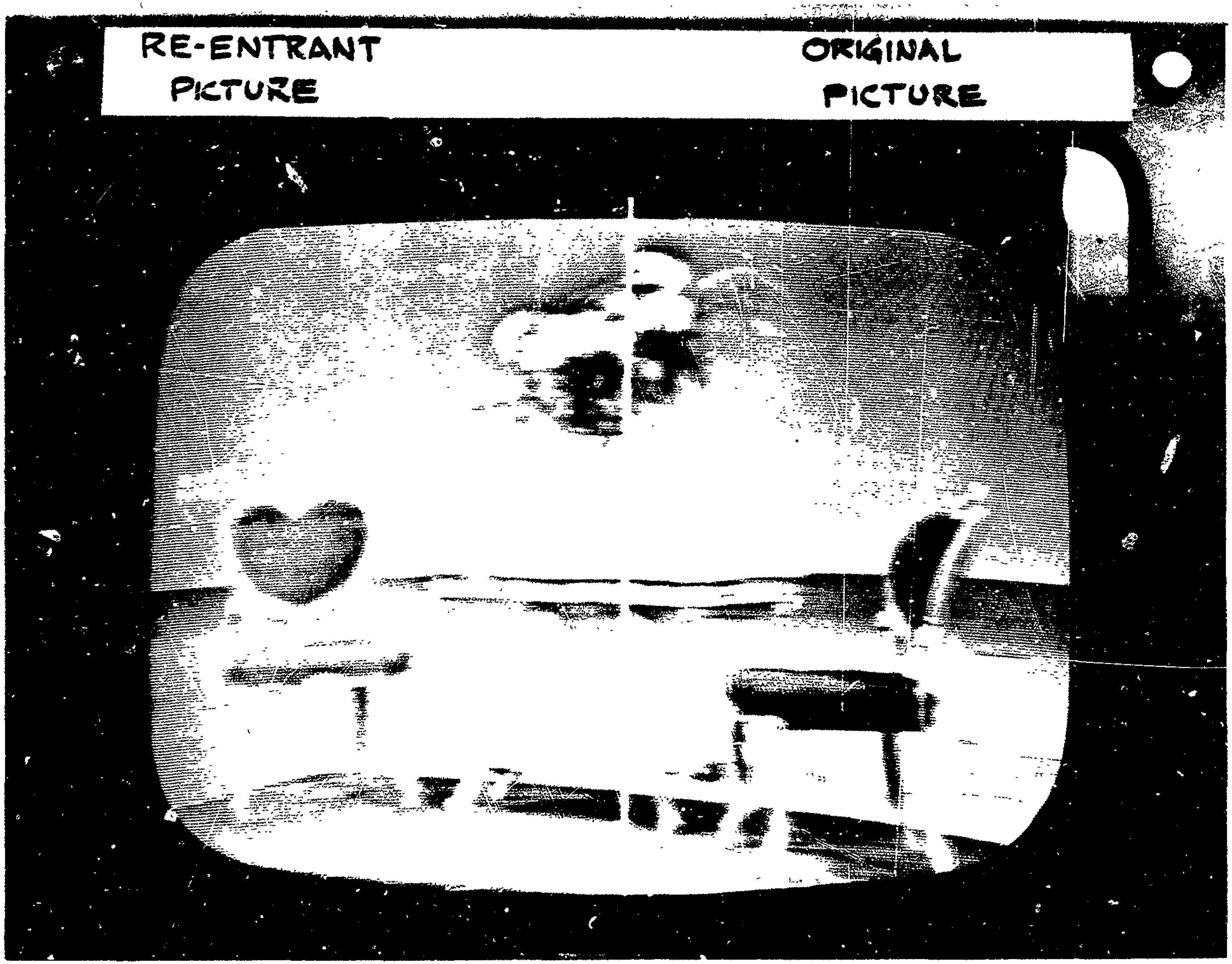

SPLIT SCREEN PRESENTATION OF WIDEBAND TV THROUGH RE-ENTRANT LOOP AND ORIGINAL VIDEO

V. DOWN CONVERTER DEVELOPMENT

The down-converter for the re-entrant TWT system is required to convert signals in the band 5.925 gc - 6.425 gc to the frequency band 3.7 gc - 4.2 gc, by means of a local oscillator of 10.125 gc. While conversion gain or slight conversion loss may be desirable, conversion loss in the vicinity of 7 to 10 db are deemed acceptable, with the restriction that the conversion loss be flat to about 0.2 db over any 50 Mc interval in the band. A desirable feature for the diplexer interface is for the converter to have the input and output signals available at a common port.

To achieve conversion gain or slight conversion loss (about 1 db), a variable capacitance diode is needed; if larger conversion losses are accepted, ordinary variable resistance mixer diodes can be used. During this period, down-converter development efforts have included investigation of varactors, tunnel diodes and variable resistance diodes. Because of the wideband requirement, sensitive matching problems presented by varactors, instabilities of tunnel diodes associated with wideband matching and uniqueness of rf to rf conversion, it was decided to concentrate on a variable resistance down-converter to provide for re-entrant loop evaluation. If time permits, development effort on the varactor down converter will be continued in parallel with the transponder evaluation and will be incorporated into the final transponder if successful.

Varactor Down-Converter

The breadboard varactor down-converter, as reported in the monthly reports, was narrowband and its gain was sensitive to mechanical vibrations. An attempt was made to integrate the stripline filters and the down-converter with relatively little improvement in the bandwidth of the converter. A completely stable varactor down-converter yielded a bandwidth of 30 Mc with 12 db of loss. The down-converter is basically a parametric amplifier with the output at the idler frequency. Hence, it is very sensitive to impedance mismatch between the converter's resonant circuits and the diplexer junction, which can produce large losses and narrowband performance. Figure 5-1 shows the gain versus pump power for the breadboard converter. The sensitivity of the gain with pump power was magnified as a result of the large initial insertion loss caused by the impedance interactions.

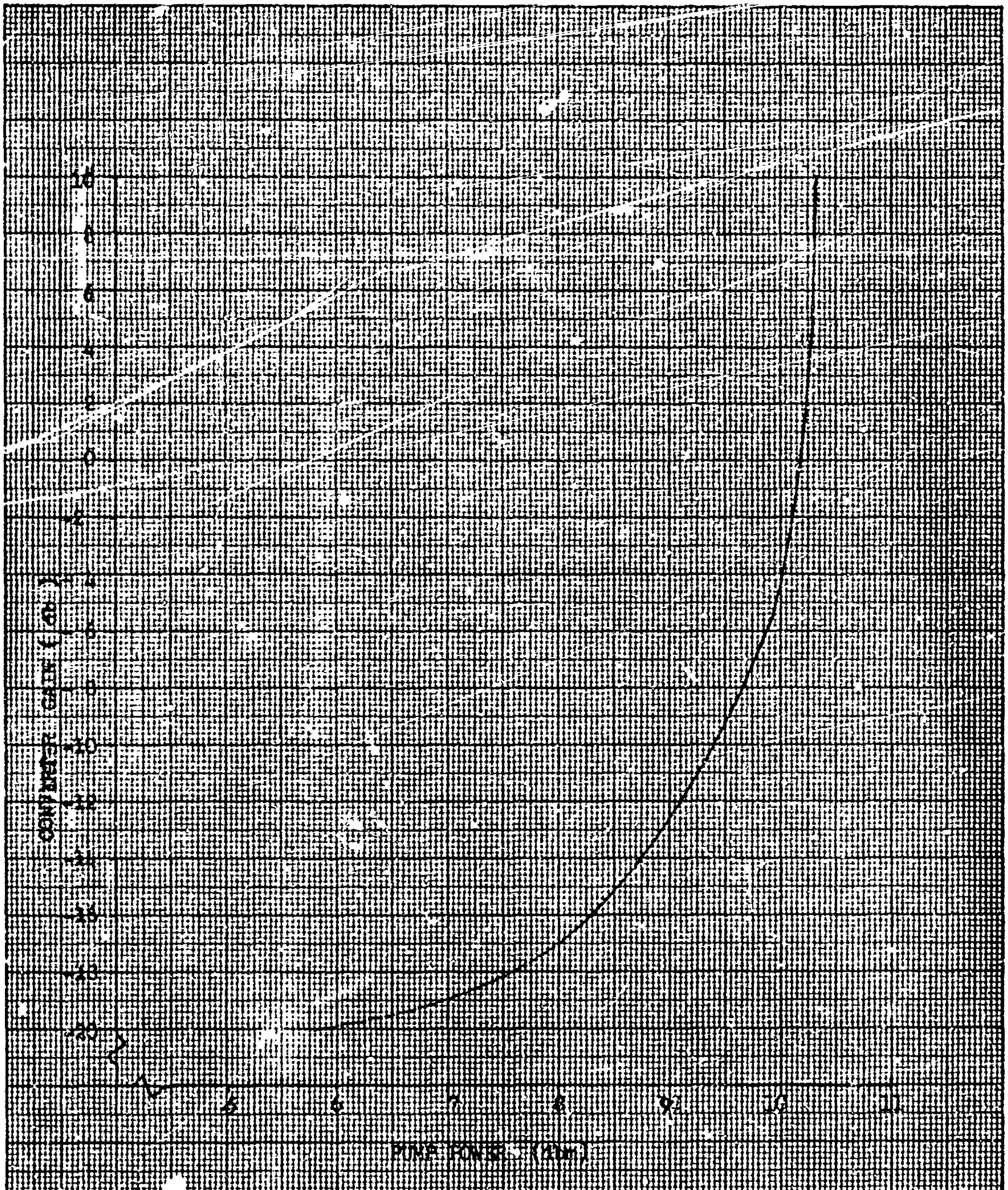

FIGURE 5.1 PUMP POWER VS VARACTOR CONVERTER GAIN

Tunnel Diode Downconverter

To overcome the bandwidth problems of a direct coupled varactor converter, a tunnel diode converter was investigated. Two tunnel diodes were purchased from Micro State Electronics Corporation.

The stability of the tunnel diode down-converter is a major problem due to the high frequencies involved and the requirement of a broadband impedance match much in excess of the two frequency bands of interest. The high cutoff frequency diodes are very susceptible to low power burnout. Thus, any unwanted oscillations are sufficient to destroy the diode before the frequency of oscillation is determined and the circuit changed. This happened to both the purchase units in the converter and the tunnel diode test circuit. Further investigation indicated that this frequently happened with the high cutoff diodes. Thus,it is felt that the tunnel diode down-converter is sufficiently difficult to stabilize such that a considerable study program would be required, which would be beyond the scope of this program.

Variable Resistance Down-Converter

The following discussion presents some semiquantatitive computations in order to suggest the design approaches taken. An equivalent circuit for a mixer diode, together with typical element values is given by:

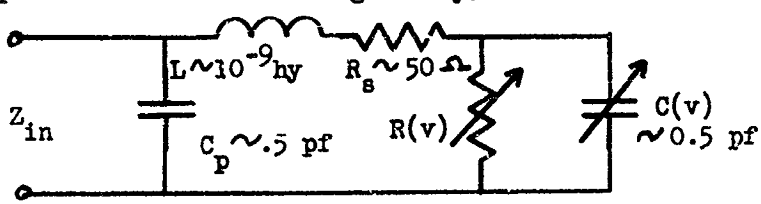

Figure 5.2 Mixer Diode Equivalent Circuit

Because of the non-linear behavior of the diode, an exact solution for Z_{in} is quite involved and will depend upon the drive level of the local oscillator, nonlinearity of $R(v)$, etc. However,it is felt that a useful approximation can be achieved by:

1) Assuming $C(v)$ to have a constant value close to its average value.
2) Assuming $R(v)$ to be either an open circuit (diode back biased and non-conducting) or a short circuit (diode forward biased and conducting).
3) Computing $Z_{in}(\infty)$ for $R(v) = \infty$ and $Z_{in}(0)$ for $R(v) = 0$ and then assuming

$$Z_{in} \simeq \frac{Z_{in}(\infty) + Z_{in}(0)}{2}.$$

The diode Z_{in}, computed as indicated above, is plotted in Figure 5-3. The resistive component is approximately 36 ohms in the 4 to 6 gc range and the reactive component is capacitive and in the order of 25 to 35 ohms over the same frequency range.

The capacitive reactance can be tuned out with a shorted transmission line, less than $\frac{\lambda}{4}$ in length, in series with the diode and the input-output port. This is the most direct approach and as indicated by Figure 5-4, it appears feasible for a single series line to give an acceptable match over the entire interval of 3.7 to 6.425 gc.

Another more involved approach, is to attempt to match only the frequency intervals of interest (i.e., 3.7 to 4.2 gc and 5.925 to 6.425 gc) without regard for mismatch outside these intervals. This case arises when a coaxial high-pass filter is employed to isolate the input-output signals from the local oscillator source. The impedance presented by this filter at the diode can exhibit an anti-resonance at a frequency between the range of interest (say at 5 gc), when a match is established at the input-output frequency bands with the aid of an auxiliary shorted transmission line in series with the diode. The reactance curves and block diagram for this approach are shown in Figure 5-5.

Breadboard models of the down-converters suggested by Figures 5-4 and 5-5 were constructed. One breadboard converter consisted of a junction between 50 ohm coaxial line and X-band waveguide. A sliding waveguide short opposite the local oscillator signal and a coaxial sliding short opposite the input-output port was used to match the diode to the input-output circuit. Unfortunately, the wideband match to the input-output signals predicted by Figure 5-4 was not observed. This was possibly due to effects of the coax-waveguide junction and prevention by the diode package itself of placing the coaxial short as close as necessary to the semiconductor element of the diode. With more work this approach may give a broadband match. However, efforts were concentrated on the breadboard realization of Figure 5-5 described below, since it initially exhibited more promise.

The breadboard suggested by Figure 5-5 consists of a mixer diode coaxially mounted in the center conductor, a low impedance series tuning line concentric with the outer conductor, and a capacitively coupled 8 pole high-pass filter.

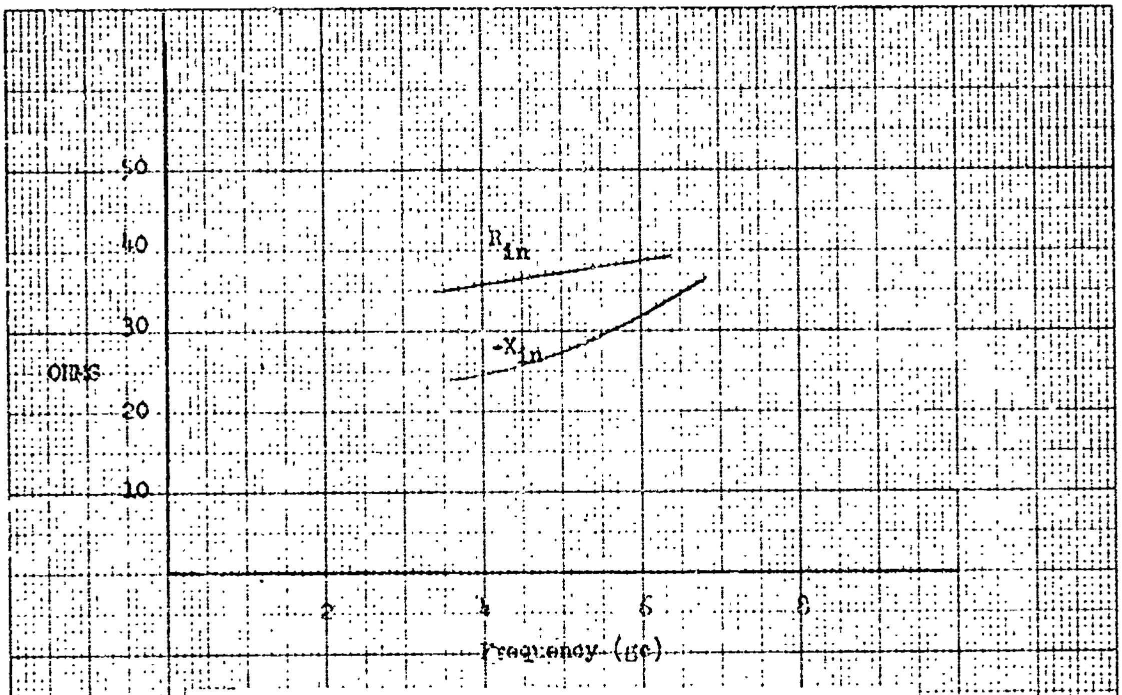

FIGURE 5.3 PUMPED DIODE IMPEDANCE COMPONENTS

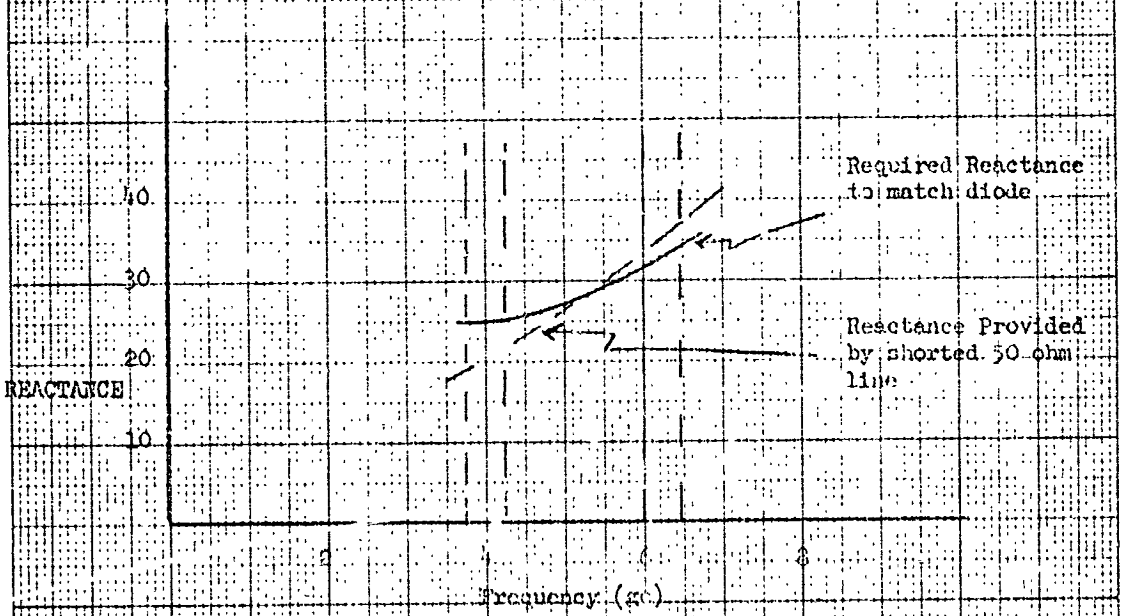

FIGURE 5.4 MATCH ATTAINED WITH SHORTED 50 OHM LINE IN SERIES WITH DIODE

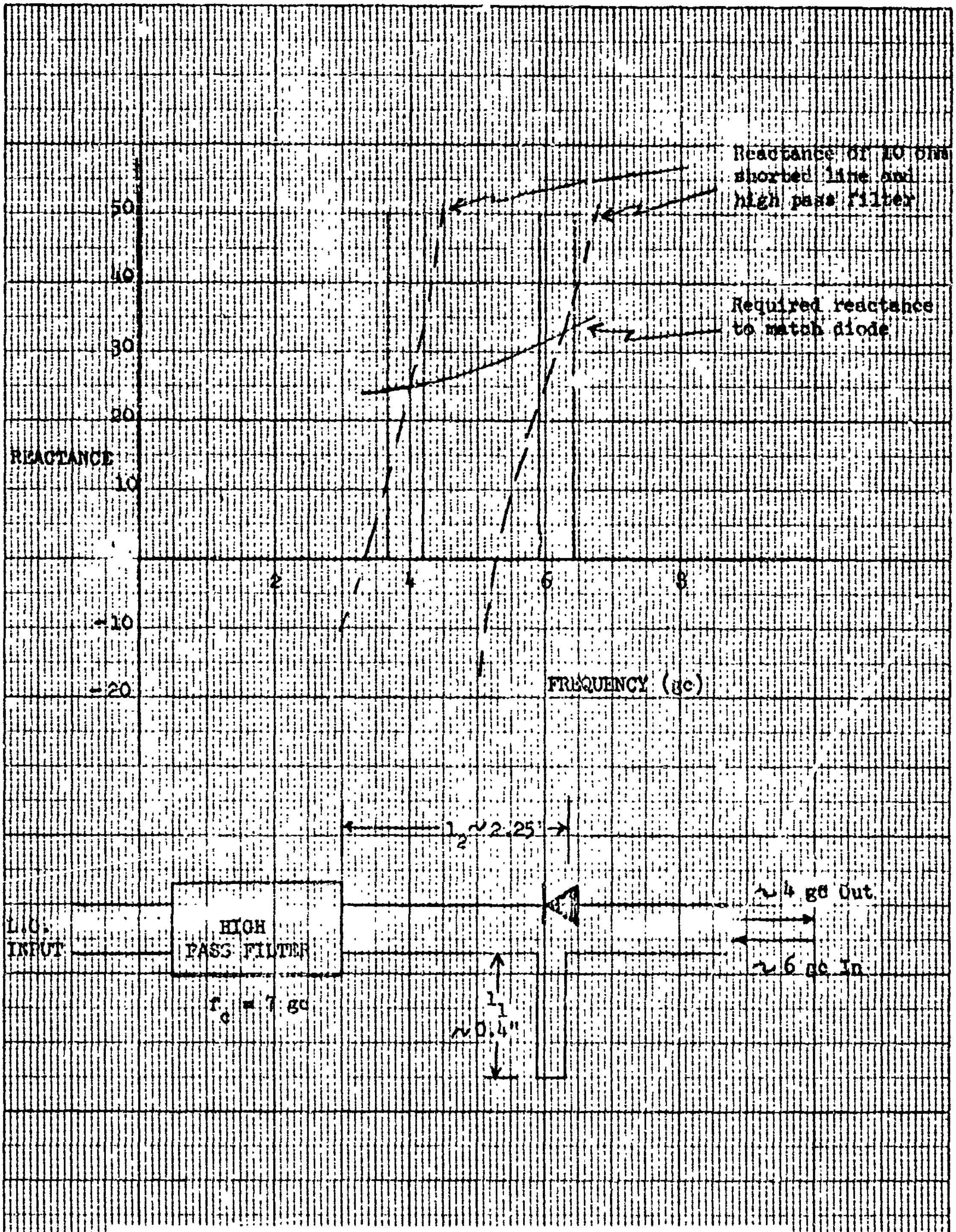

FIGURE 5.5 COAXIAL CONVERTER REACTANCE CURVES

The data obtained on the device is shown in Figure 5-6. Conversion loss ranged from 6 db to 9.5 db over the 3.7 to 4.2 output frequency band. Also shown in Figure 5-6 is VSWR data and a curve formed by adding the reflection losses at the output frequencies and their corresponding input frequencies to an assumed 4 db crystal conversion loss which is superimposed on the measured conversion loss data.

Similar results were obtained for several diodes of the 1N415 and 1N416 types. The data shown in Figure 5-6 was taken with a 500 ohm resistor in the dc return for self-biasing of the diode, which then required 4 to 8 milliwatts of local oscillator power to yield the lowest conversion loss. When the biasing resistor was replaced with a direct short, the conversion loss increased by 1/2 db, while the required local oscillator power dropped by 3 db.

A prototype model of the all coaxial converter has been constructed, as shown in Figure 5-7, and present efforts are directed towards a flat wideband response. In addition, work on the waveguide-coax junction converter, shown in Figure 5-8, will continue in parallel.

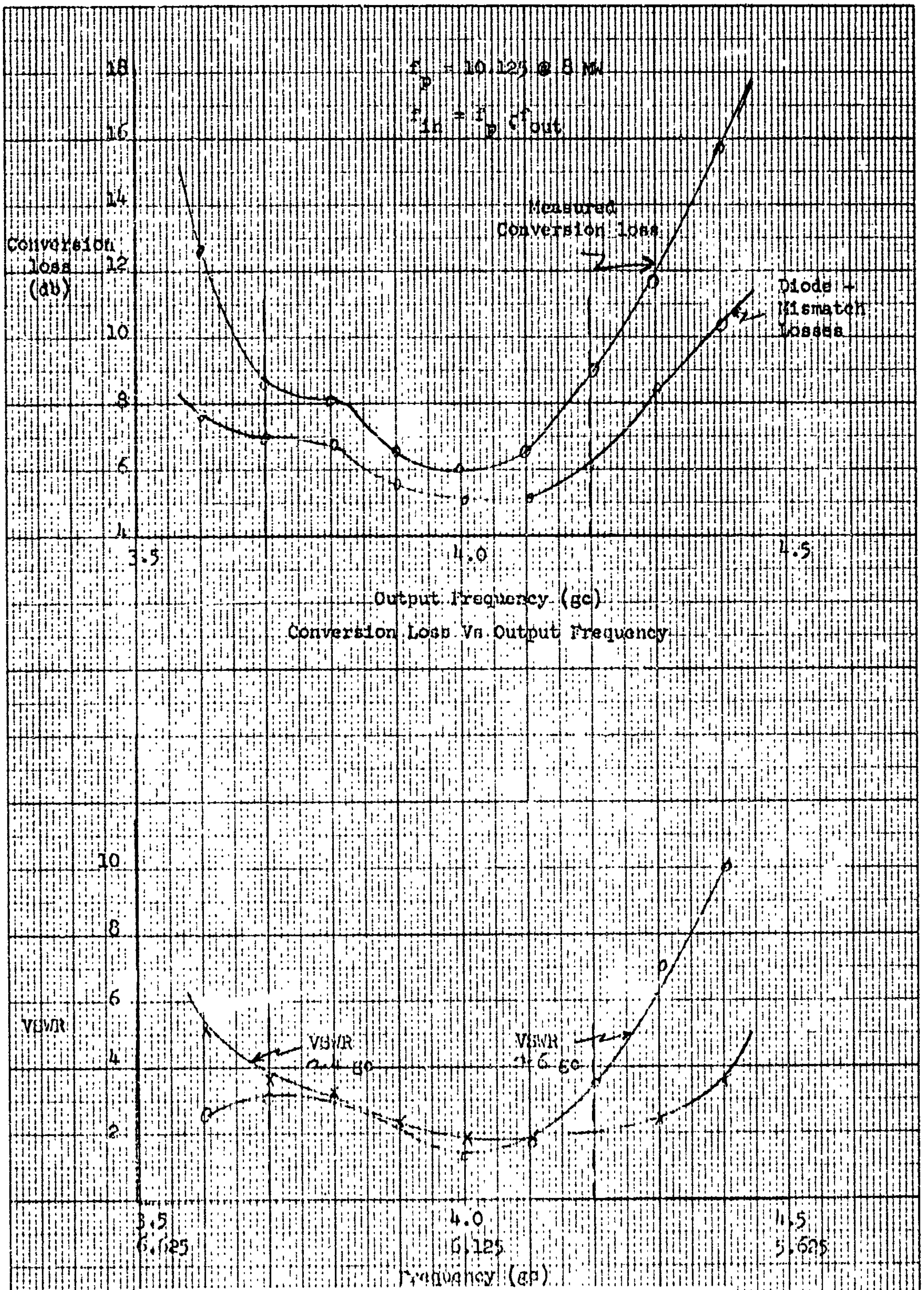

FIGURE 5.6 DATA ON COAXIAL CONVERTER (1N416F)

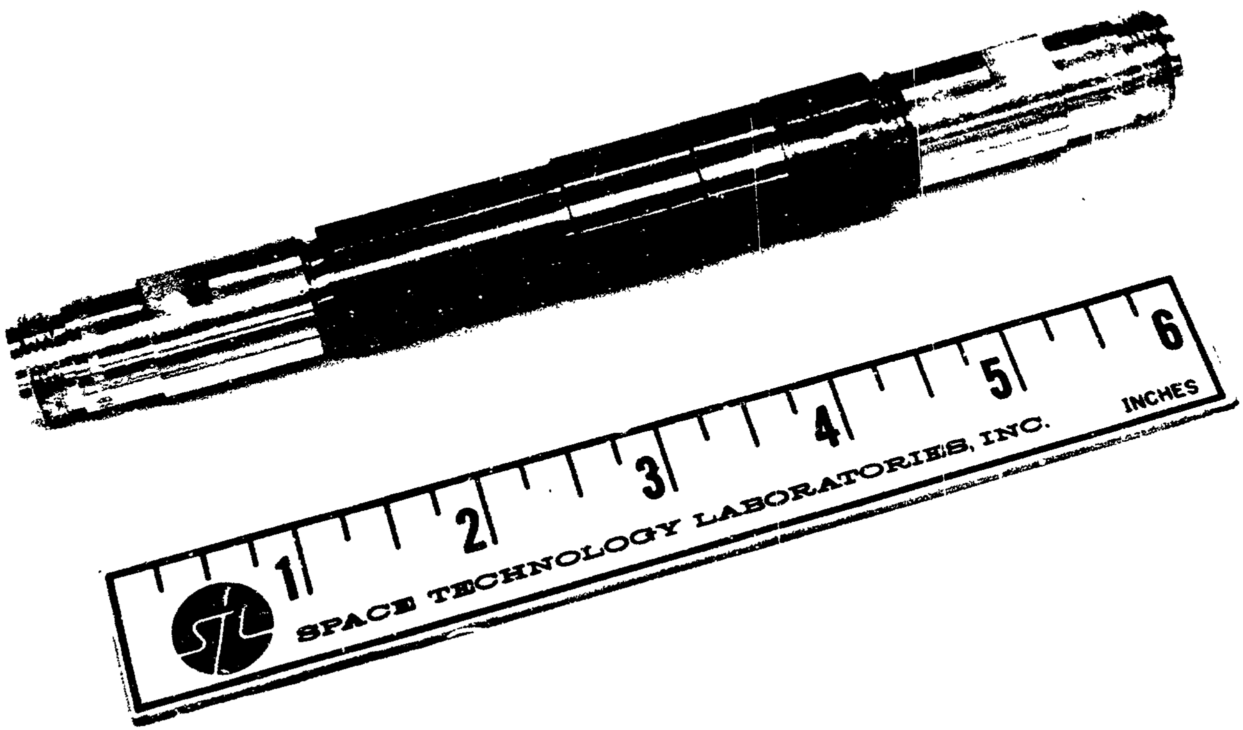

FIGURE 5-7   COAXIAL DOWN-CONVERTER

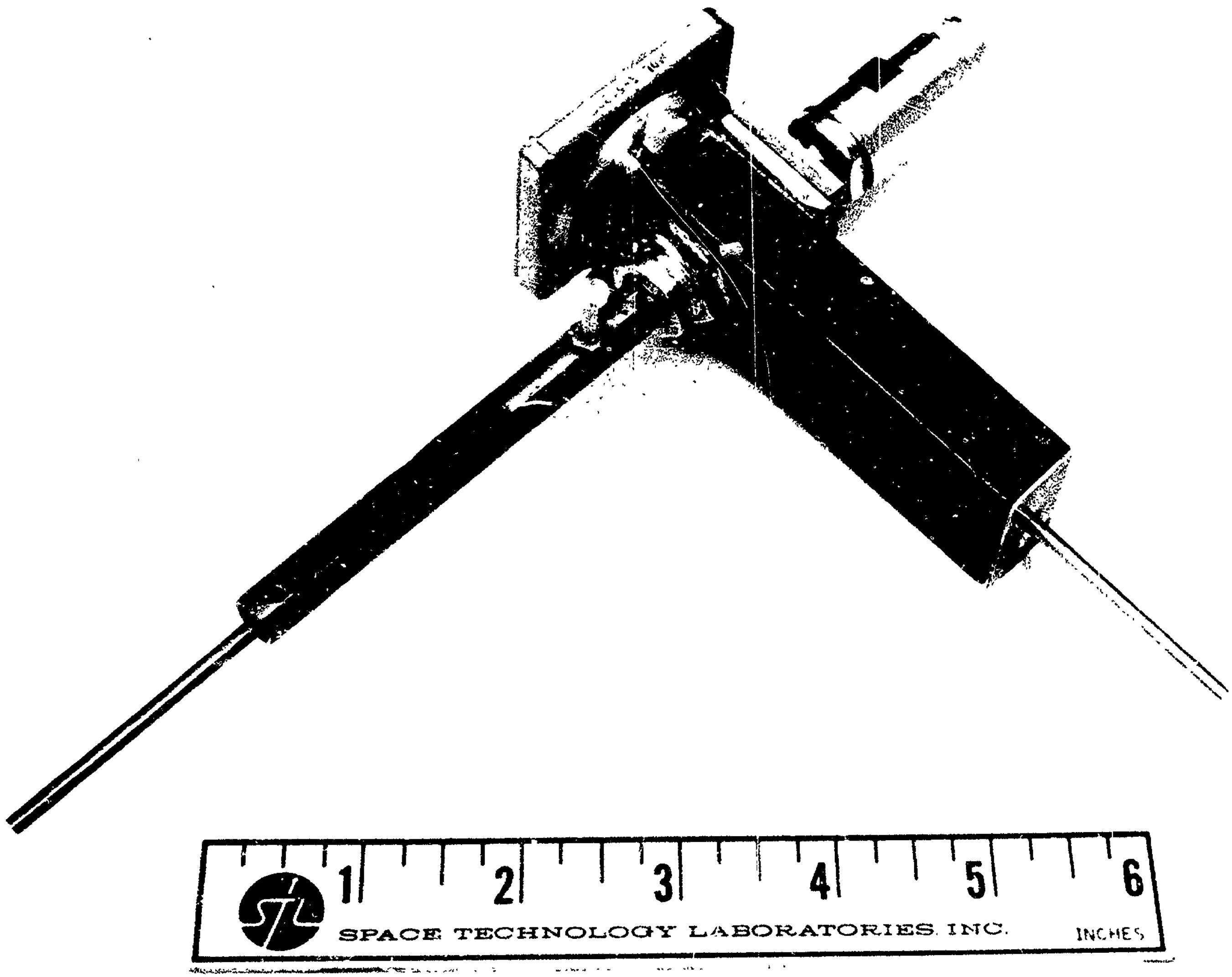

FIGURE 5-8 WAVEGUIDE-COAX DOWN CONVERTER

VI. PROGRAM FOR NEXT QUARTER

The effort for the fourth and final quarter will include the following:

1. Completion of down-converter development
2. Completion of intermodulation analysis
3. Empirical evaluation of the Re-entrant amplifier
4. Completion of Re-entrant transponder
5. Empirical evaluation of total transponder
6. Analytical evaluation of empirical results
7. Package breadboard transponder
8. Specification, drawing and equipment release
9. Initiate final report.

VII. REFERENCES

1. International Radio Consultative Committee (CCIR), "Documents of the IXth Plenary Assembly, Los Angeles, 1959 (Second Impression 1960)," Volume I, Recommendations, p. 268.

2. J. A. Develet, Jr., "Coherent FDM/FM Telephone Communication," Proc. IRE, September, 1962.

APPENDIX A

INTERFERENCE BETWEEN PM WAVES

In most of the preceding analysis of interference we required an expression for the interference spectrum which appears at baseband. That is, since the transmission objectives for the relay are stated in terms of equivalent noise falling in the worst baseband telephone channel, we must know the interference spectrum both to determine the worst channel and to compute the interference noise. In this Appendix we develop formulas for the spectral density of the interference at baseband and indicate a method for the practical computation of the interference products which is due to Curtis.[1]

The sum of two phase-modulated waves is

$$A_1 \cos \left[\omega_1 t + \phi_1(t) + \alpha_1\right] + A_2 \cos \left[\omega_2 t + \phi_2(t) + \alpha_2\right]$$

in which A_1, A_2, ω_1 and ω_2 are constants, α_1 and α_2 are random variables, each uniformly distributed on $[-\pi, \pi]$, and $\phi_1(t)$ and $\phi_2(t)$ are assumed to be sample functions of two independent wide-sense stationary Gaussian random processes having zero means. The sum can be expressed in the well-known alternative form

$$A(t) \cos \left[\omega_1 t + \alpha_1 + \phi_1(t) + \theta(t)\right] , \tag{1}$$

where $\phi_1(t)$ is now assumed to be the desired information-bearing signal and, for $A_2/A_1 << 1$,

$$\theta(t) = \frac{A_2}{A_1} \sin \left[(\omega_2 - \omega_1) t + \alpha + \phi_2(t) - \phi_1(t)\right] \tag{2}$$

where $\alpha = \alpha_2 - \alpha_1$.

After perfect limiting and phase detection, the output signal is $\alpha_1 + \phi(t_1) + \theta(t)$. The power spectral density of this composite random process can be found, if it exists, as the Fourier transform of the covariance function of the process.

For the baseband power spectrum to exist, the process must be at least second-order stationary. We examine the first mean of the process $\alpha_1 + \phi_1(t) + \theta(t)$ for stationarity:

$$
\begin{aligned}
E\left[\alpha_1 + \phi_1(t) + \theta(t)\right] &= E\,\alpha_1 + E\,\phi_1(t) + E\,\theta \\
&= E\,\theta(t) \\
&= E\,\frac{A_2}{A_1}\sin\left[(\omega_2 - \omega_1)t + \alpha + \phi_2(t) - \phi_1(t)\right] \\
&= \frac{A_2}{A_1}\left\{E\sin\left[\Delta\omega t + \phi_2 - \phi_1\right]E\cos\alpha + E\cos(\Delta\omega t + \phi_2 - \phi_1)\,E\sin\alpha\right\} \\
&= 0 \quad \text{since } E\cos\alpha = E\sin\alpha = 0.
\end{aligned}
$$

Note that $\omega_2 - \omega_1$ has been redefined as $\Delta\omega$. The desired process is therefore at least first order stationary.

Since the first mean of the process is zero, the covariance function and the autocorrelation function are identical. Therefore,

$$R(t_1, t_2) = E\left[a_1 + \phi_1(t_1) + \theta(t_1)\right]\left[a_1 + \phi_1(t_2) + \theta(t_2)\right]$$

$$= E\,\phi_1(t_1)\,\phi_1(t_2) + E\,\phi_1(t_1)\,\theta(t_2) + E\,\phi_1(t_2)\,\theta(t_1)$$

$$+ E\,\theta(t_1)\,\theta(t_2) + E\,a_1^{\,2} \qquad (3)$$

$$= R_{\phi_1}(t_1, t_2) + R_{\phi_1\theta}(t_1, t_2) + R_{\theta\phi_1}(t_1, t_2)$$

$$+ R_\theta(t_1, t_2) + E\,a_1^{\,2}$$

since $E\,a = 0$ and a is independent of $\phi_1(t)$ and $\theta(t)$. The first term is the autocorrelation function of the desired information process $\phi_1(t)$ and it should be noted that $R_{\phi_1}(t_1, t_2) = R_{\phi_1}(t_1 - t_2) = R_{\phi_1}(\tau)$, because $\phi_1(t)$ is assumed stationary. The remaining terms represent various forms of distortion due to the interfering signal. The cross-correlation terms take the form

$$R_{\phi_1\theta}(t_1, t_2) = E\left\{\phi_1(t_1)\frac{A_2}{A_1}\sin\left[\Delta\omega t_2 + a + \phi_2(t_2) - \phi_1(t_2)\right]\right\}$$

$$= \frac{A_2}{A_1}\,E\cos a\,E\left\{\phi_1(t_1)\sin\left[\Delta\omega t_2 + \phi_2(t_2) - \phi_1(t_2)\right]\right\}$$

$$+ \frac{A_2}{A_1}\,E\sin a\,E\left\{\phi_1(t_1)\cos\left[\Delta\omega t_2 + \phi_2(t_2) - \phi_1(t_2)\right]\right\}$$

$$= 0$$

That is, the processes $\phi_1(t)$ and $\theta(t)$ are uncorrelated. The only distortion term is therefore $R_\theta(t_1, t_2)$. This term may be evaluated as follows:

$$R_\theta(t_1, t_2) = \left(\frac{A_2}{A_1}\right)^2 E\left\{\sin\left[\Delta\omega t_1 + \alpha + \phi_2(t_1) - \phi_1(t_1)\right]\right.$$
$$\left.\sin\left[\Delta\omega t_2 + \alpha + \phi_2(t_2) - \phi_1(t_2)\right]\right\}$$
$$= \frac{1}{2}\left(\frac{A_2}{A_1}\right)^2 E\left\{\cos(\Delta\omega\tau + \Delta\phi_2 - \Delta\phi_1)\right. \tag{4}$$
$$\left.- \cos\left[\Delta\omega(t_1 + t_2) + 2\alpha + \Sigma\phi_2 - \Sigma\phi_1\right]\right\}$$
$$= \frac{1}{2}\left(\frac{A_2}{A_1}\right)^2 E\cos(\Delta\omega\tau + \Delta\phi_2 - \Delta\phi_1)$$

in which $\tau = t_1 - t_2$, $\Delta\phi = \phi(t_1) - \phi(t_2)$, $\Sigma\phi = \phi(t_1) + \phi(t_2)$
The last result (4) can be conveniently evaluated by noting that

$$E\cos(\Delta\omega\tau + \Delta\phi_2 - \Delta\phi_1) = \frac{1}{2}e^{i\Delta\omega\tau}\, E\exp(i\Delta\phi_2)\, E\exp(-i\Delta\phi_1)$$
$$+ \frac{1}{2}e^{i\Delta\omega t}\, E\exp(-i\Delta\phi_2)\, E\exp(i\Delta\phi_1)$$
$$= \frac{1}{2}e^{i\Delta\omega t}\, M_2(i1, -i1)\, M_1(-i1, i1)$$
$$+ \frac{1}{2}e^{-1\Delta\omega t}\, M_2(-i1, i1)\, M_1(i1, -i1)$$
$$= M_1(i1, -i1)\, M_2(i1, -i1)\cos\Delta\omega\tau \tag{5}$$

In the above, the joint characteristic function of the random variables $\phi(t_1)$ and $\phi(t_2)$ has been introduced:

$$M(iV_1, iV_2) = E\exp i\left[V_1\,\phi(t_1) + V_2\,\phi(t_2)\right]$$

For Gaussian random variables[2] with zero means and variances σ_1^2, σ_2^2,

$$M(iV_1, iV_2) = \exp - \frac{1}{2}\left[\sigma_1^2 V_1^2 + 2\sigma_1\sigma_2\rho V_1 V_2 + \sigma_2^2 V_2^2\right],$$

and

$$M(i1, -i1) = \exp - \sigma^2(1-\rho) = \exp - \left[R(o) - R(\tau)\right].$$

Finally, then, we have for the distortion term,

$$R_\theta(\tau) = \frac{1}{2}\left(\frac{A_2}{A_1}\right)^2 \exp - \left[R(o) - R(\tau)\right] \cos \Delta\omega\tau, \qquad (6)$$

where $R(\tau) = R_1(\tau) + R_2(\tau)$ and $R_1(\tau)$, $R_2(\tau)$ are the autocorrelation functions of the processes $\phi_1(t)$, $\phi_2(t)$.

The autocorrelation function of the random phase process of the equivalent carrier has therefore been shown to be stationary. Furthermore, the desired phase information $\phi_1(t)$ and the phase distortion $\theta(t)$ have been shown to be uncorrelated processes. The autocorrelation function of the phase output or baseband signal is $R_{\phi_1}(\tau) + R_\theta(\tau)$. The one-sided spectral intensity of the interference can now be found as the Fourier transform of $R_\theta(\tau)$.

$$W(f) = 4\int_0^\infty R_\theta(\tau) \cos 2\pi f\tau \, d\tau$$

$$= 2\left(\frac{A_2}{A_1}\right)^2 e^{-R(o)} \int_0^\infty e^{R(\tau)} \cos \Delta\omega\tau \cos 2\pi f\tau \, d\tau \qquad (7)$$

Thus, in principle, if the autocorrelation function of the baseband processes $\phi_1(t)$ and $\phi_2(t)$ are known the spectrum of the interference as manifested at baseband can be calculated from (7). However, a more practical method of calculating the interference spectrum will now be demonstrated.

If two phase-modulating signals are $\phi_1(t)$ and $\phi_2(t)$ and their autocorrelation functions are $R_{\phi_1}(\tau)$ and $R_{\phi_2}(\tau)$, Stewart[3] has shown that the autocorrelation function of the modulated signal is

$$R(\tau) = \frac{A^2}{2} \cos \omega \tau \; e^{-\left[R_\phi(o) - R_\phi(\tau)\right]} \tag{8}$$

It can be seen, therefore, that by multiplying the autocorrelation functions of the RF signals one obtains

$$R_1(\tau)\, R_2(\tau) = \frac{A_1^2 A_2^2}{4} \cos \omega_1 \tau \cos \omega_2 \tau \; e^{-R(o)} \, e^{R(\tau)}$$

$$R_1(\tau)\, R_2(\tau) = \frac{A_1^2 A_2^2}{8} e^{-R(o)} \, e^{R(\tau)} \left[\cos \Delta\omega\tau + \cos(\omega_1 + \omega_2)\tau\right], \tag{9}$$

where $\quad R(\tau) = R_{\phi_1}(\tau) + R_{\phi_2}(\tau).$

If we take (9) to be a new autocorrelation function, and solve for the power spectrum, we find

$$W(f) = \frac{A_1^2 A_2^2}{2} \int_0^\infty e^{-R(o)} \, e^{R(\tau)} \cos \Delta\omega\tau \cos 2\pi f \tau \, d\tau$$

$$+ \frac{A_1^2 A_2^2}{2} \int_0^\infty e^{-R(o)} \, e^{R(\tau)} \cos(\omega_1 + \omega_2)\tau \cos 2\pi f \tau \, d\tau \tag{10}$$

If the desired carrier power is normalized to unity $\left(A_1^2/2 = 1\right)$, then the first term of (10) is seen to be just the result achieved in (7) for the power spectrum of the baseband interference. The second term yields that portion of the power spectrum located at the frequency

$$(\omega_1 + \omega_2)/2\pi$$

which is of no interest in the baseband interference problem and may be disregarded. The importance of this result is that it allows the calculation of the baseband interference spectrum by the convolution of the spectra of the RF signals as demonstrated.

FOOTNOTES

1. H. E. Curtis, "Interference Between Satellite Communication Systems and Common Carrier Surface Systems," Bell System Technical Journal, Volume 40, May 1962, p. 11.

2. W. B. Davenport, Jr., and W. L. Root, An Introduction to the Theory of Random Signals and Noise, McGraw-Hill, 1958, p. 149.

3. J. L. Stewart, "The Power Spectrum of a Carrier Frequency Modulated by Gaussian Noise," Proc. IRE, 42 (October 1954); pp. 1539-1542.